Performance Evaluation of HVAC Systems via Coupled Simulation between Modelica and OpenFOAM

Qiao, H.; Nabi, S.; Laughman, C.R.

TR2019-073 July 25, 2019

Abstract

High-performance building design heavily relies on computational models that can predict the dynamic interactions between HVAC equipment, air flow and building envelope. This paper presents a coupled simulation of Modelica and OpenFOAM to evaluate the system performance of a room air-conditioner operating in buildings. The dynamic models of the air-conditioner are constructed in Modelica, whereas the indoor airflow is simulated in OpenFOAM. Dynamic system characteristics are analyzed and compared against those obtained with the well-mixed air model. The effects of thermal stratification and thermostat placement on the system energy efficiency are also discussed.

International Conference on Compressor and Refrigeration

Performance Evaluation of HVAC Systems via Coupled Simulation between Modelica and OpenFOAM

Hongtao QIAO*, Saleh NABI and Christopher R. LAUGHMAN

Mitsubishi Electric Research Laboratories, Cambridge, MA 02139 USA

{qiao, nabi, laughman}@merl.com

Keywords: Coupled simulation, Modelica, CFD, HVAC systems, OpenFOAM, Refrigeration cycle.

Abstract High-performance building design heavily relies on computational models that can predict the dynamic interactions between HVAC equipment, air flow and building envelope. This paper presents a coupled simulation of Modelica and OpenFOAM to evaluate the system performance of a room air-conditioner operating in buildings. The dynamic models of the air-conditioner are constructed in Modelica, whereas the indoor airflow is simulated in OpenFOAM. Dynamic system characteristics are analyzed and compared against those obtained with the well-mixed air model. The effects of thermal stratification and thermostat placement on the system energy efficiency are also discussed.

Introduction

The building sector is facing significant and growing challenges related to its impacts on energy consumption and global warming. In the U.S., buildings account for about 42% of primary energy usage, 73% of electricity consumption, and over 40% of carbon emissions. The largest part of the energy usage in buildings is related to the HVAC systems, which consist of components working together to introduce, distribute and condition air for human comfort and refrigeration. Therefore, improving the energy efficiency of HVAC systems has been an active area of research.

Computational modeling and simulation has been proven conducive to design of high energy-efficient HVAC systems because it can facilitate the exploration of complex system characteristics without requiring expensive and laborious construction of experimental platforms. Models that are capable of predicting transient behavior of HVAC systems can be used for advanced and optimal control design, which could yield a significant reduction in daily energy consumption of buildings and more comfortable and healthier indoor environments for occupants. However, modeling and simulation of HVAC systems in buildings is very challenging and requires deep fundamental knowledge in multidisciplinary domains because these are large, complex systems that are governed by dynamics on many different time and length scales with many different levels of interaction.

Building Performance Simulation (BPS) has been playing an important role in new building and retrofit design, code compliance, green certification, and real-time building control. A BPS program primarily focuses on three physical domains, i.e., heat, air and moisture, based on the input information which includes a description of building geometry, construction materials, lighting, HVAC, control strategies, and operating details. Such a program often uses local weather data and calculates thermal loads and resulting energy use as well as occupant comfort based on the first-principles equations. Since BPS tools are typically used for the assessment of the thermal performance of buildings over the course of an entire year, they generally are based on the simplified analysis for air flow, heat and moisture transport. For instance, indoor air is often assumed to be well-mixed and non-uniform distributions of velocity, temperature, pressure and concentration are neglected. This assumption can be justified when it comes to predicting the performance of buildings with small space, but might lead to erroneous results for large buildings with thermal stratification. In addition, this assumption cannot satisfy advanced design requirements, such as personal cooling/heating and optimal sensor placement, due to lack of local thermal comfort information [1].

In contrast with the well-mixed assumption, computational fluid dynamics (CFD) divides fluid domain into a large number of small volumes and solves the conservation equations in three dimensions, yielding a detailed prediction of velocity, temperature, pressure and humidity ratio distributions. Meanwhile, CFD conducts high-resolution analyses near boundary walls, which leads to more accurate heat transfer prediction. Theoretically, CFD can be applied to the simulation of the whole building including its envelope, but it is extremely computationally expensive due to the conjugate heat transfer problem which involves heat transfer in both solid and fluid. Given the capabilities and deficiencies of individual programs, it is a no-brainer to consider integrating BPS with CFD in a way that BPS models weather data, building envelope, HVAC systems and control algorithms, and provides boundary conditions to CFD, whereas CFD simulates the indoor airflow dynamics based on the provided boundary conditions and then sends the average airflow and temperature/heat transfer information back to BPS such that a closed-loop analysis is accomplished.

Given that CFD simulation generally is quite time-consuming, there is an emerging interest in replacing full-scale CFD simulation for indoor environment with Fast Fluid Dynamics (FFD) due to its superior computational efficiency [2]. However, due to its simplified scheme and the assumption of constant turbulent viscosity, FFD can lead to significant deviations in predicting air flow dynamics under certain conditions. Meanwhile, FFD does not support unstructured mesh and thus cannot deal with complex geometry. Furthermore, FFD presumes that heat source is uniformly distributed in space and therefore is unable to handle non-uniform heat source/sink. All these disadvantages have restricted FFD from being broadly applied to air flow simulation within the building community.

For the sake of brevity, a detailed literature review on the coupled simulation of BPS and CFD is not given here. Interested readers are referred to [3]. It is worthwhile to point out that all reported coupled simulations unanimously focus on integration of air handler units with indoor environment, and never take into account the effect of refrigerant systems, which are the essential part of HVAC systems and the primary energy consumer. Without incorporating refrigerant systems into the coupled analysis, it is impossible to accurately predict building energy performance. Meanwhile, feedback control design of such systems requires accounting for the complex dynamic characteristics of phase-changing refrigerant flows, which are affected by air flows inside buildings. Therefore, it is necessary to include refrigerant systems in the simulation to perform more comprehensive analyses. Another observation through literature review is that these co-simulation studies are all based on the commercial CFD programs, e.g., Fluent, CFX and STAR-CD. These programs are generally expensive and the source code is inaccessible. Hence, development of a middleware that couples commercial CFD programs with BPS requires non-trivial efforts.

To bridge the research gap, we have developed a coupled simulation platform using Modelica and OpenFOAM. Modelica is an equation-oriented modeling language and has been gaining in popularity for the modeling of complex thermo-fluid systems due to its object-oriented acausal modeling approach, whereas OpenFOAM is a well-recognized open-source CFD engine that provides users full access to its source code. In this platform, dynamic models in the Modelica language have been developed to model HVAC systems including refrigeration cycles, building envelope and control algorithms, while OpenFOAM is used to simulate indoor environment. With this platform, the pull-down performance of a room air-conditioner with different vane angles and airflow modes were explored [4]. As a continuation of our previous work, this presented paper aims to evaluate the system performance of a room air-conditioner operating on the hottest day of Chicago in a year. The overall system dynamics will be compared with those obtained with the well-mixed air model. In addtion, the effects of thermostat placement on the system performance will be analyzed.

The remainder of the paper is organized as follows. In the second section, the data exchange mechanism between Modelica and OpenFOAM is presented. In the third section, we describe a variety of models that are used to construct the whole eco-system model. In the fourth section, we use the controlled system model to run the simulations and analyze the system performance. Conclusions from this work are then summarized in the final section.

Data Exchange Mechanism in Co-Simulation

Data cannot be directly transferred between Modelica and OpenFOAM, and a middleware interface is required to facilitate data exchange. Specifically, both Modelica and OpenFOAM communicate with the middleware, which stores and transfers data from and to both programs. In general, the computational speed of BPS models changes during the simulation and is much faster than that of CFD models, therefore, a fixed synchronization time step for data exchange between two programs needs to be predefined. The synchronization time step usually should be larger than the integration time steps of the respective programs, which can be either fixed or adaptive. A quasi-dynamic data synchronization scheme is used in the coupled simulation, i.e., two programs only exchange data between each other at synchronization and keep their received data unchanged between synchronizations.

When the Modelica simulation reaches the synchronization point, it will halt the current execution and check whether or not the old Modelica data, i.e., CFD boundary conditions, have been read by OpenFOAM. If yes, Modelica will transfer the new Modelica data to the middleware and wait for the new CFD data from OpenFOAM to be available. If not, Modelica will keep waiting until the old Modelica data are read by OpenFOAM. The new Modelica data will be written to file, i.e., data.in, and will be read by OpenFOAM as the new CFD boundary conditions for the subsequent simulation.

OpenFOAM uses its built-in *externalCoupled* function object which provides a file-based communication interface to transfer data to and from OpenFOAM [5]. The data exchange employs specialized boundary conditions to provide either uni- or bi-directional models. At start-up, the *externalCoupled* function creates a lock file, i.e., OpenFOAM.lock, to signal the external source, i.e., the middleware in this case, to wait. When the OpenFOAM simulation reaches synchronization, new Modelica boundary conditions are written to file, i.e., data.out. Then the lock file is removed and OpenFOAM will halt its execution, instructing the middleware to take control of the program execution. The middleware will read the new CFD data from data.out and transfer them to Modelica. When ready, the middleware will re-instate the lock file and pass program execution back to OpenFOAM. The *externalCoupled* function will then read the new CFD boundary conditions from data.in, and resume the simulation.

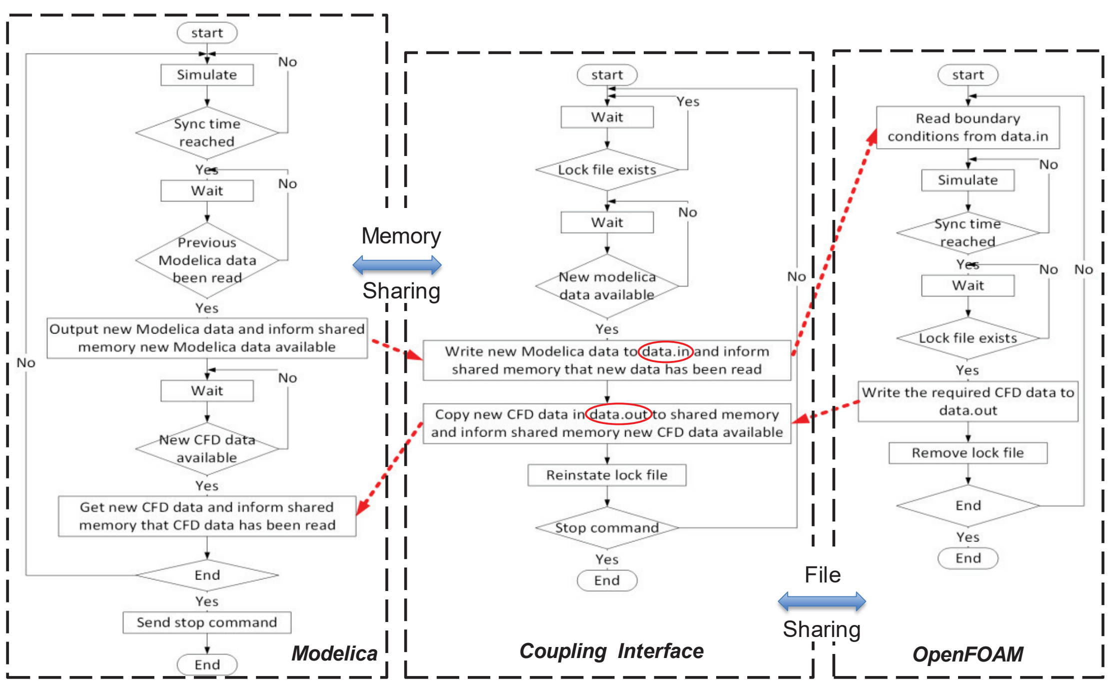

Fig. 1 Data exchange process in the coupled simulation

Zuo et al. (2016) [2] developed a coupled simulation between FFD and the Modelica Buildings library for the dynamic ventilation system with stratified air distribution. In our work, we retained their implementation within Modelica and between Modelica and the middleware, but made significant changes in both the middleware and OpenFOAM such that data transfer between the middleware and OpenFOAM can take place. The detailed process for data exchange between Modelica and OpenFOAM is shown in Fig. 1.

Models

The studied air-conditioning system consists of two main parts: the outdoor unit and the indoor unit. The outdoor unit is installed on or near the wall outside of the room or space that you wish to cool. The outdoor unit houses the compressor, condenser, whereas the indoor unit contains the evaporator, expansion device, a blower fan and an air filter. Fig. 2 illustrates the schematic of a typical air-conditioning system. As the system models have been described at length in previous publications, we emphasize only the details of these models needed to provide sufficient context for this paper.

Component Models The temporal behavior of the refrigeration cycle is dominated by the heat exchangers over the time scales of seconds to hours, so the system models in this work used dynamic models of the heat exchangers and static (algebraic) models of the compressor and expansion valve. We assume 1-D flow for the refrigerant so that properties only vary along the length of the pipes; we also assume that the refrigerant can be described as a Newtonian fluid, negligible viscous dissipation and axial heat conduction in the direction of flow, negligible contributions to the energy equation from the kinetic and potential energy of the refrigerant, negligible dynamic pressure waves in the momentum equation, and thermodynamic equilibrium in each volume for which the refrigerant is in the two-phase region.

Under these assumptions, the partial differential equations describing the conservation of mass, momentum, and energy for the refrigerant can be spatially discretized to construct a set of finite volume models [6, 7]. A staggered grid scheme is used to avoid nonphysical pressure variations caused by numerical artifacts by decoupling the mass and energy equations computed for the volume cells from the momentum equations computed for the flow cells. Integration of these equations across these cells, as well as the use of the upwind difference method to approximate refrigerant properties for the convection-dominated flows from this application, results in a set of ordinary differential equations describing the conservation equations, as given in Eqs. (1), (2), and (3).

$$A_c \Delta z \left(\frac{\partial \bar{\rho}_i}{\partial p_i} \frac{dp_i}{dt} + \frac{\partial \bar{\rho}_i}{\partial \bar{h}_{\rho,i}} \frac{d\bar{h}_{\rho,i}}{dt} \right) = \dot{m}_{i-1/2} - \dot{m}_{i+1/2} \tag{1}$$

$$A_c \left(p_{i+1} - p_i \right) = P \Delta z \bar{\tau}_{w,i+1/2} \tag{2}$$

$$A_c \Delta z \left(\bar{\rho}_i \frac{d\bar{h}_{\rho,i}}{dt} - \frac{dp_i}{dt} \right) = \dot{m}_{i-1/2} \left(h_{i-1/2} - \bar{h}_{\rho,i} \right) - \dot{m}_{i+1/2} \left(h_{i+1/2} - \bar{h}_{\rho,i} \right) + P \Delta z q_i'' \tag{3}$$

where $\bar{h}_\rho$ and $\bar{h}$ signify the density-weighted and flow-weighted specific enthalpies, the wall shear stress $\bar{\tau} = \frac{1}{2} f \bar{\rho} u |u|$ and f is the Fanning friction factor, and P is the circumference of the flow channel. These symbols with overbars represent average quantities in each cell. Pressure p and density-weighted specific enthalpy $\bar{h}_\rho$ are used as dynamic states in the models.

A set of simplified closure relations for the frictional pressure drop and the refrigerant-side heat transfer coefficients were used because many correlations from the literature have poor numerical properties that make them unsuitable for inclusion in a dynamic simulation. The frictional pressure drop was expressed as $\Delta p / \dot{m}^2 = \kappa \left(\Delta p_0 / \dot{m}_0^2 \right)$, where the empirical correlations were used to determine the nominal values of κ and Δp_0. Simplified heat transfer relations for each phase were also used in which the heat transfer coefficient for each phase was only dependent upon refrigerant mass flow rate, and the smooth transition between the phases was enforced [8].

A multicomponent moist-air model was used for the air-side of this work, in which both dry air and water vapor were described by ideal gas equations. The mass and energy conservation equations used to describe the heat transfer from the outer surface of the tubes to the air reflected this multicomponent model, as described by Eq. (5), where the mass transfer coefficient was given by a modified Lewis correlation.

$$\dot{m}_a c_{p,a} \frac{dT_a}{dy} \Delta y = \alpha_a \left(A_{o,t} + \eta_{fin} A_{o,fin} \right) \left(T_w - T_a \right) \tag{4}$$

$$\dot{m}_a \frac{d\omega_a}{dy} \Delta y = \alpha_m \left(A_{o,t} + \eta_{fin} A_{o,fin} \right) \min\left(0, \omega_{\mathrm{w},sat} - \omega_a \right) \tag{5}$$

A simple isenthalpic model of the electronic expansion valve was also used, as described by a standard orifice flow equation

$$\dot{m} = C_v \sqrt{\rho_{in} \Delta p} \tag{6}$$

where the mass flow rate is regularized in the neighborhood of zero flow to prevent the derivative of the mass flow rate from tending toward infinity. The flow coefficient C_v is generally determined via calibration against experimental data.

The cycle models in this work included a variable-speed low-side scroll compressor, in which the motor is cooled by the low-pressure refrigerant entering the compressor. Due to the complex nature of the heat transfer and fluid flow through the compressor, we used simplified 1-D models of this component to parsimoniously describe the system. The behavior of the compressor was described by relating the volumetric efficiency η_v and isentropic efficiency η_isen to the suction pressure p_suc, discharge pressure p_dis, and compressor frequency ϖ, as given by

$$\eta_v = \dot{m} / \left(\rho_{suc} V_{disp} \varpi \right) \tag{7}$$

$$\eta_{isen} = \left(h_{dis,isen} - h_{suc} \right) / \left(h_{dis} - h_{suc} \right) \tag{8}$$

The compressor power consumption was also related to the compressor speed and the ratio of inlet and outlet pressures. The coefficients used for the functional forms of η_v and η_isen were derived from experimental data, and the expressions are provided in [9].

Standard fan laws [10] were used to describe the behavior of the heat exchanger fans. According to such models, the volumetric flow rate was assumed to be directly proportional to the fan speed, while the power consumed by the fan was assumed to be proportional to the cube of the fan speed. These simple algebraic models were scaled by experimentally measured values of fan speed, flow rate, and power; to minimize the error in these fits, linear and quadratic terms were also included in the power model to account for observed variations in the data.

Building Model Unlike the cycle models used in this work, the building models were based upon the open-source Modelica Buildings library [11], an extensive and well-tested library of components for the construction of dynamic building and building system models.

The room model from the Buildings library are based on the physics-based behavior of the fundamental materials and components commonly used in the building construction industry. These individual materials are parameterized by fundamental properties like thickness, thermal conductivity, and density, and can be combined and assembled into multi-layer constructions. The accuracy of the multi-layer models is ensured by automating the discretization of the partial differential equations representing heat transfer in the materials by using the Fourier number to ensure that the time constants of each volume are approximately equal.

However, the zone air model incorporated into the room model is a mixed air single-node model with one bulk air temperature that interacts with all of the radiative surfaces and thermal loads in the room. As indicated previously, such a well-mixed air model can result in significant deviations for building performance prediction. Therefore, we used CFD to model the heat and mass transfer in the indoor environment, which will be described shortly.

This building is constructed on a 0.1meter thick concrete slab, with a constant soil temperature of 15 °C, while the exterior surfaces were assumed to have an absorptivity of 0.9. This building was located in Chicago, IL, USA, and the corresponding TMY3 weather file was used to drive the model with realistic solar and thermal boundary conditions to understand the detailed room thermal dynamics. The space was assumed to contain 800 W of sensible load and 425 W of latent load.

CFD Model CFD toolbox OpenFOAM was selected to simulate airflow dynamics in the buildings. We modified the solver buoyantPimpleFoam [5], available in the 2.3.0 version of OpenFOAM, to account for the simultaneous heat and moisture transport in space. Furthermore, we constructed time-varying boundary conditions to enable data transfer between Modelica and OpenFOAM during the coupled simulation.

Considering the compressibility, the conservation equations of mass, momentum and energy are

$$\frac{\partial \rho}{\partial t}+\nabla\cdot\left(\rho\vec{u}\right)=0 \tag{9}$$

$$\frac{\partial}{\partial t}\left(\rho\vec{u}\right)+\nabla\cdot\left(\rho\vec{u}\vec{u}\right)=-\nabla p+\rho\vec{g}+\nabla\cdot\left(2\mu_{eff}D\left(\vec{u}\right)\right)-\nabla\left(\frac{2}{3}\mu_{eff}\left(\nabla\cdot\vec{u}\right)\right) \tag{10}$$

$$\frac{\partial}{\partial t}\left(\rho h\right)+\nabla\cdot\left(\rho\vec{u}h\right)+\frac{\partial}{\partial t}\left(\rho K\right)+\nabla\cdot\left(\rho\vec{u}K\right)-\frac{\partial p}{\partial t}=\nabla\cdot\left(\alpha_{eff}\nabla h\right)+\rho\vec{u}\cdot\vec{g}+S_h \tag{11}$$

where the rate of strain tensor $D\left(\vec{u}\right)$ is defined as $D\left(\vec{u}\right)=\frac{1}{2}\left(\nabla\vec{u}+\left(\nabla\vec{u}\right)^T\right)$. ρ and h are the density and specific enthalpy of moist air, defined as $\rho = (1 - Y)\rho_a + Y\rho_w$ and $h = [(1 - Y)c_{p,a} + Y c_{p,w}](T - T_0)$, respectively. The effective thermal diffusivity α_{eff} is the sum of laminar and turbulent thermal diffusivities. Moisture transport needs to be taken into account in the simulation, and the convection-diffusion equation is described as

$$\frac{\partial\left(\rho Y\right)}{\partial t}+\nabla\cdot\left(\rho\vec{u}Y\right)=\nabla\cdot\left(\rho D_{eff}\nabla Y\right)+S_i \tag{12}$$

where Y is the concentration of moisture, and D_{eff} is the sum of laminar and turbulent diffusion coefficients. In Eqs. (11) and (12), S_h and S_i are the volumetric heat source and volumetric rate of water vapor creation, respectively. To define a volumetric source, a membership function is used to determine whether a cell is entirely, partially inside or completely outside the cube (enclosed by $[x_{min}, x_{max}]$, $[y_{min}, y_{max}]$ and $[z_{min}, z_{max}]$) occupied by the source. Based on the value of ϕ, one can compute the source term S for the entire fluid domain.

$$\begin{aligned}\phi &= \phi_x\phi_y\phi_z\\ \phi_x &= \left\{\tanh\left[k\left(x-x_{\min}\right)\right]-\tanh\left[k\left(x-x_{\max}\right)\right]\right\}/2\\ \phi_y &= \left\{\tanh\left[k\left(y-y_{\min}\right)\right]-\tanh\left[k\left(y-y_{\max}\right)\right]\right\}/2\\ \phi_z &= \left\{\tanh\left[k\left(z-z_{\min}\right)\right]-\tanh\left[k\left(z-z_{\max}\right)\right]\right\}/2\end{aligned} \tag{13}$$

Results and Discussion

The models described in the previous section were assembled into an overall system model and simulated eight-hour operation in Chicago from 9:00 am to 5:00 pm on July 19th to evaluate its system performance. The air conditioning system used R410A as the working fluid. The compressor had a displacement of 6.8 cm^3 and nominal rotational speed of 3500 rpm, and both heat exchangers were louvered fin-and-tube heat exchangers. The indoor unit was installed in the center of the west wall in a room with dimensions of 5 × 5 × 2.6 m (length × width × height), as shown in Fig. 3. To avoid complicated mesh, the indoor unit was simplified as a cube with the supply vent and return vent on the bottom and the top, respetively. Two feedback loops closed on the suction superheat and room temperature, driving the opening of the electronically actuated expansion valve and compressor frequency, respectively. The suction superheat setpoint was 2 K and room temperature was set to 26 °C. The heat source was located in a cube with demensions of 1 × 2.8 × 1 m ($x_{\min}$ = 3.5m, $x_{\max}$ = 4.5m, $y_{\min}$ = 1.1m, $y_{\max}$ = 3.9m, $z_{\min}$ = 0.2m and $z_{\max}$ = 1.2m), while the water vapor source was located in a smaller cube with dimensions of 1 × 2.8 × 0.2 m ($x_{\min}$ = 3.5m, $x_{\max}$ = 4.5m, $y_{\min}$ = 1.1m, $y_{\max}$ = 3.9m, $z_{\min}$ = 1.0m and $z_{\max}$ = 1.2m). The initial air temperature and relative humidity in the room was 32 °C and 80%, respectively. The vane angle and air flow mode of the indoor unit was set to 45° and medium, respectively.

During the simulation, Modelica models for air-conditioner determined the air temperature, velocity and water vapor concentration at the inlet for the CFD model, while CFD calculated air temperature and water vapor concentration at the outlet for the Modelica models. Meanwhile, Modelica building envelope models provided the average surface temperatures of interior walls to CFD, while CFD calculated the heat flux for the building envelope models. The synchronization time step was set to 10 sec. The Modelica models were implemented using the Dymola 2019 simulation environment. The simulation was performed on a desktop with an Intel i7-2600 processor with 4 cores and 8 Gb of RAM, and the ratio of the physical time to the CPU time was approximately 1:3. The solver settings and boundary conditions for the CFD room model were summarized in Table 1.

Three simulation experiments were carried out to compare the system performance of the air-conditioner with different room models and different thermostat placement: (1) Center air temperature control - this simulation used CFD room model and the thermostat was located in the room center; (2) Return air temperature control - this case also used the CFD room model, but the thermostat was placed at the return vent of the indoor unit; (3) Well-mixed air model - this case used the well-mixed air model of the Buildings library with all other settings the same as the previous two cases. The location of thermostat did not matter in the third case since air temperature was assumed to be uniform in the room. All the pertinent results were presented and disccused below.

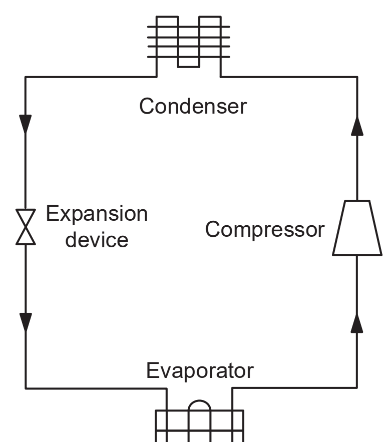

Fig. 2 Air-conditioning system

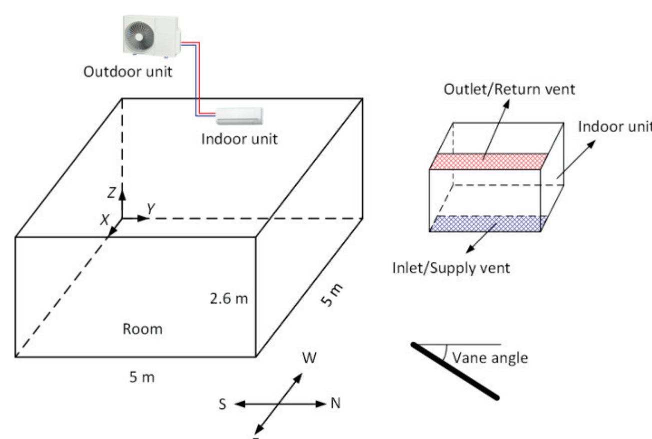

Fig. 3 CFD calculation domain

Table 1. Solver settings and boundary conditions of CFD room model

Item	Content
Turbulence model	k-epsilon model
Time dependent	Transient simulation (Courant number < 1), Δt = 0.01s
Inlet boundary condition	Time-varying $\vec{u}$, T and Y
Outlet boundary condition	Time-varying $\vec{u}$, zeroGradient for T and Y
Wall boudary conditions	Time-varying T, no-slip for $\vec{u}$, zeroGradient for Y
Mesh size	7648
Solver	Modified buoyantPimpleFoam

With the same control gains for all cases, room temperature settled down at the setpoint after around 3 hours, as shown in Fig. 4a. However, the CFD model led to larger undershoot in room temperature than the well-mixed air model, indicating that the latter introduced more damping to the system and might not be well suited for control design. The compressor frequency transients given in Fig. 4b evidently demonstrated that the system could run with very different compressor speeds even if the controlled target was achieved. With the CFD model, lower compressor frequency was required for the center air temperature control than the return air temperature control, yielding more than 10% higher energy efficiency, as shown in Fig. 4c. This manifested that thermostat placement had a remarkable effect on the system performance. Because thermal stratification existed in the room due to the gravity effect, return air temperature control could lead to overcooling the space given that the return vent was generally close to the ceiling. Therefore, proper placement for thermostat not only can help achieve comfort temperature for occupants, but also can improve the system performance.

Relative humidity of the return air was also compared in Fig. 4d for three cases. Similar transients were observed, indicating that water vapor distribution did not exhibit such a pronouced stratification phenomenon as air temperatures did. Fig. 4e to 4g illustrated the heat transfer rate from the interior walls to the room air. In the first two cases with CFD model, the floor rejected the most heat to the room air because (1) the temperatures of the air above the floor were the lowest, and (2) the jet flow from the indoor unit impinged upon the floor, resulting in the much higher heat transfer coefficients. Because CFD conducts high-resolution analyses near boundary walls and can provide more accurate heat transfer calculations, one should not be surprised that substantial differences were observed between Fig. 4e, 4f and 4g. The thermal stratification in the room for different thermostat placement was shown in Fig. 4h. For either thermostat placement, air temperatures at three different elevations (0.1m, 1.3m and 2.5m) were compared. It was evident that air temperature increased with elevation and air temperature near the floor could be 2 °C lower than that near the ceiling. Meanwhile, when the thermostat was placed at the return vent of the indoor unit, the average room temperature was about 1.3°C lower than that when the thermostat was located in the center of the room. This difference corraborated that the compressor needed to run more aggressively in the second case due to an increase in thermal load, resulting in lower system efficiency.

Conclusions

This paper demonstrated a coupled simulation of Modelica and OpenFOAM to evaluate the system performance of a room air-conditioner operating in the summer of Chicago. The overall system dynamics were compared with those obtained with the well-mixed air model. It was demonstrated that the use of coupled simulation with detailed CFD model for indoor environment facilitates more accurate exploration of system dynamics than using the well-mixed air model due to thermal stratification in space. Meanwhile, simulations indicated that thermostat placement could impose pronounced impact on the energy performance of HVAC systems. Future work will include the optimization of thermostat placement to maximize the energy efficiency of HVAC systems while maintaining the thermal comfort in space.

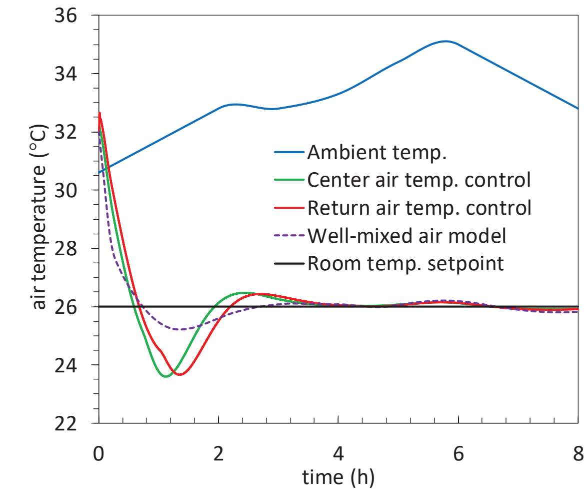

36
34
32
30
28
26
24
22
0
2
4
6
8
air temperature (°C)
time (h)
Ambient temp.
Center air temp. control
Return air temp. control
Well-mixed air model
Room temp. setpoint

(a)

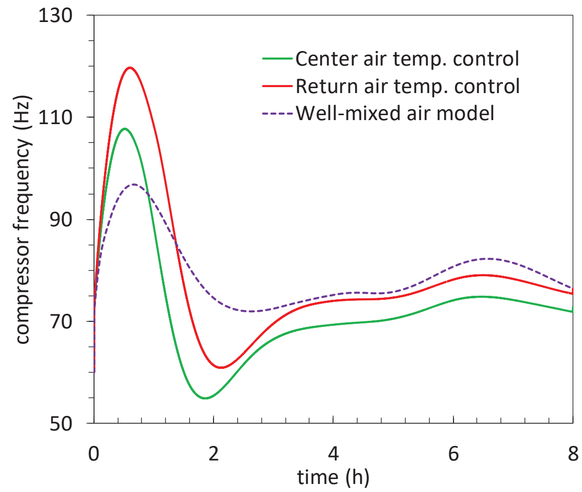

130
110
90
70
50
0
2
4
6
8
compressor frequency (Hz)
time (h)
Center air temp. control
Return air temp. control
Well-mixed air model

(b)

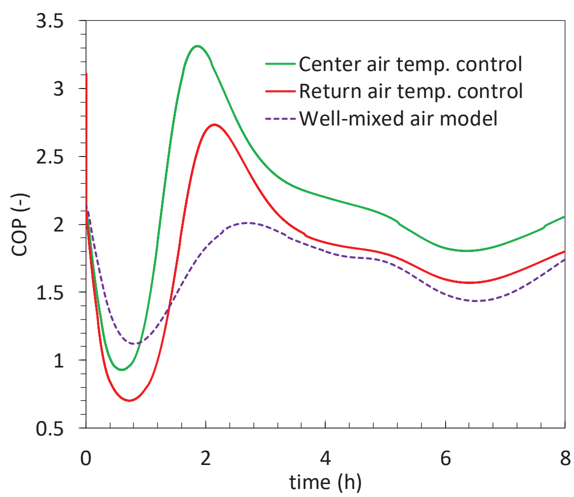

3.5
3
2.5
2
1.5
1
0.5
0
2
4
6
8
COP (-)
time (h)
Center air temp. control
Return air temp. control
Well-mixed air model

(c)

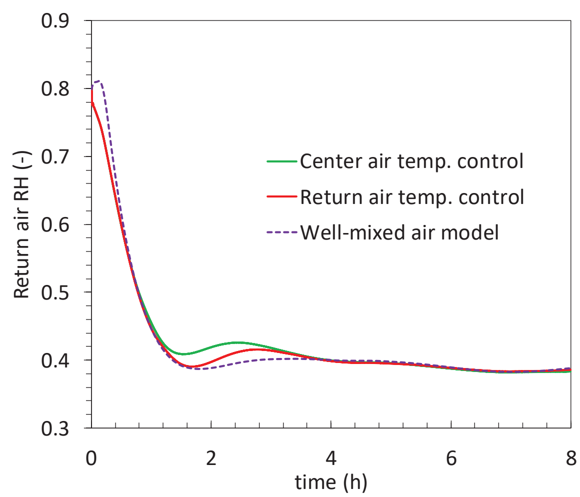

0.9
0.8
0.7
0.6
0.5
0.4
0.3
0
2
4
6
8
Return air RH (-)
time (h)
Center air temp. control
Return air temp. control
Well-mixed air model

(d)

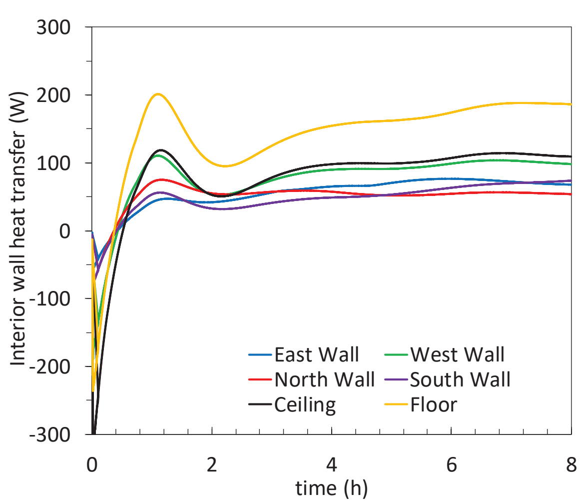

300
200
100
0
-100
-200
-300
0
2
4
6
8
Interior wall heat transfer (W)
time (h)
East Wall
West Wall
North Wall
South Wall
Ceiling
Floor

(e)

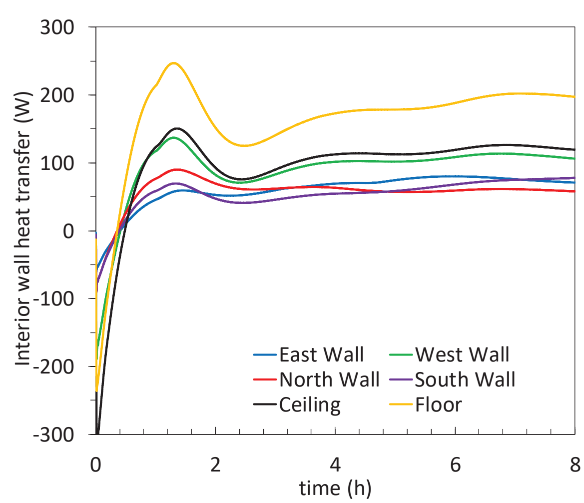

300
200
100
0
-100
-200
-300
0
2
4
6
8
Interior wall heat transfer (W)
time (h)
East Wall
West Wall
North Wall
South Wall
Ceiling
Floor

(f)

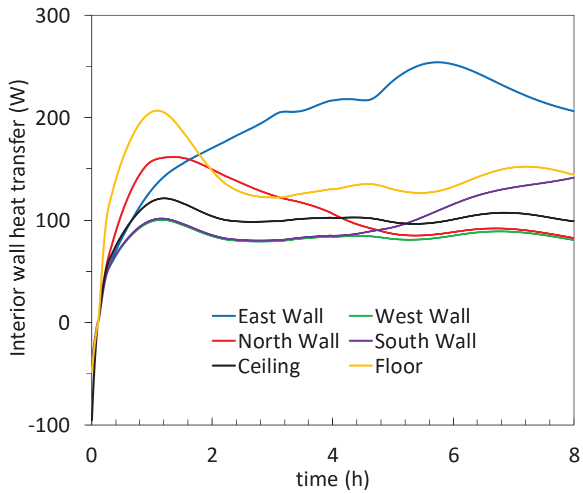

(g)

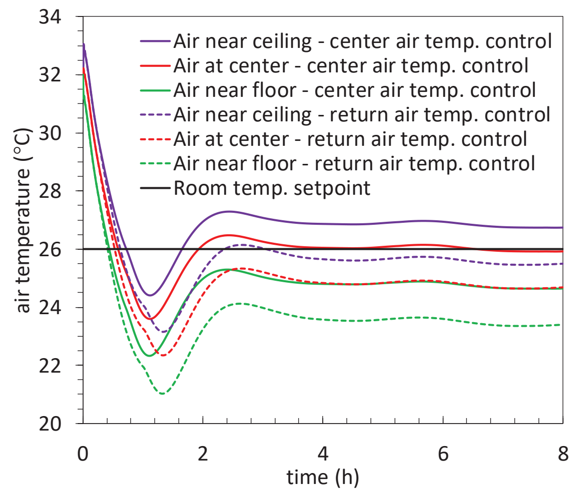

(h)

Fig. 4 (a) - room air temperature transients; (b) - compressor frequency transients; (c) - COP of room air-conditioner; (d) - return air relative humidity transients; (e) - heat rejection from interior walls to room air for center air temperature control; (f) - heat rejection from interior walls to room air for return air temperature control; (g) - heat rejection from interior walls to room air for well-mixed air model; (h) - thermal stratification in the room

References

[1] S. Nabi, P. Grover, C.P. Caulfield, Adjoint-based optimization of displacement ventilation flow, Build. Environ. 124 (2017) 342-356.

[2] W. Zuo, M. Wetter, W. Tian, D. Li, M. Jin, Q. Chen, Coupling indoor airflow, HVAC, control and building envelope heat transfer in the Modelica Buildings library, J. Build. Perform. Simu. 9 (2016) 366-381.

[3] W. Tian, X. Han, W. Zuo, M.D. Sohn, Building energy simulation coupled with CFD for indoor environment: a critical review and recent applications, Energ. Buildings 165 (2018) 184-199.

[4] H. Qiao, H. Xu, S. Nabi, C.R. Laughman, Coupled simulation of a room air-conditioner with CFD models for indoor environment, 13th International Modelica Conference, OTH Regensburg, Germany, 2019.

[5] OpenFOAM Foundation, https://github.com/OpenFOAM/ /OpenFOAM-dev.

[6] H. Qiao, V. Aute, R. Radermacher, Transient modeling of a flash tank vapor injection heat pump system - part I: model development, Int. J. Refrig. 49 (2015) 169–182.

[7] H. Qiao, C.R. Laughman, Comparison of approximate momentum equations in dynamic models of vapor compression systems, 16th International Heat Transfer Conference, Beijing, China, 2018.

[8] C.R. Laughman, H. Qiao, On closure relations for dynamic vapor compression cycle models, American Modelica Conference, Boston, MA, 2018.

[9] H. Qiao, C.R. Laughman, D. Burns, S. Bortoff, Dynamic characteristics of an R410A multi-split variable refrigerant flow air-conditioning system, 12th IEA Heat Pump Conference, 2017.

[10] ASHRAE, HVAC Systems and Equipment Handbook, ASHRAE, Atlanta, GA, 2008

[11] M. Wetter, W. Zuo, T.S. Nouidui, X. Pang, Modelica Buildings Library, J. Build. Perform. Simu. 7 (2014) 253-270.